Journal of Materials Chemistry A

Accepted Manuscript

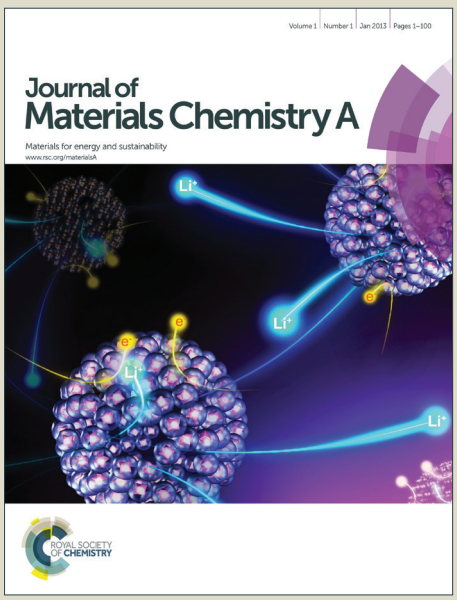

ROYAL SOCIETY OF CHEMISTRY

www.rsc.org/materialsA

aSynthesis and Characterization of Triptycene-Based Polyimides with Tunable High Fractional Free Volume for Gas Separation Membranes

Jennifer R. Wiegand[a], Zachary P. Smith[b], Qiang Liu[b], Christopher T. Patterson[a], Benny D. Freeman[b], Ruilan Guo[a,*]

[a]*University of Notre Dame, Department of Chemical and Biomolecular Engineering, Notre Dame, IN 46556*

[b]*University of Texas at Austin, Center for Energy and Environmental Resources, Department of Chemical Engineering, Austin, TX 78758, United States*

* Corresponding author, +1-574-631-3453 (tel), +1-574-631-8366 (fax), rguo@nd.edu

Abstract

Robust polymer membranes that are highly permeable and selective are desired for energy efficient gas separation processes. In this study, a series of rigid, bulky triptycene-based diamine monomers were designed, synthesized, and subsequently incorporated into the backbone of polyimides via polycondensation with 2,2'-bis-(3,4-dicarboxyphenyl) hexafluoropropane dianhydride (6FDA) to obtain a series of polyimide membranes with high fractional free volume. These triptycene-containing polyimides with systematic variations in their chemical structure demonstrate the viability of 'tunable' fractional free volume by introducing various substituents onto the polymer backbone. All the polyimides synthesized exhibited film-forming high molecular weight, high solubility, and excellent thermal properties, with glass transition temperatures ranging from 280 °C to 300 °C and thermal stability up to 500 °C. Compared to other classes of glassy polymers, these triptycene-polyimides had high combinations of permeability and selectivity, suggesting that a favorable free volume size distribution in these triptycene polyimides was induced by the unique chain packing mechanism of triptycene units. The correlation between gas transport properties with the polymer chemical structure was also investigated. Altering the size of the substituents neighboring the triptycene units provides greater opportunity to fine-tune the fractional free volume and free volume size distribution in the polymer, which in turn can change the transport properties effectively to meet various separation needs. It is expected that additional design modifications made by exploiting the chemistry versatility of triptycene moiety and by selectively adding other components may improve these membranes to break the gas permeability-selectivity trade-off barrier.

Keywords: triptycene, polyimide, tunable fractional free volume, gas separation membranes

Introduction

Many industrial processes involve separation of small gas molecules. Some examples include the production of nitrogen-enriched air for food packaging, hydrogen separations for syngas ratio adjustment, and carbon dioxide removal for natural gas sweetening, among others[1]. Polymeric membrane-mediated gas separation has emerged as an important and fast-growing separation technology that has potential advantages in cost and energy efficiency, and reduced environmental impact over traditional separation processes such as cryogenic distillation, thermal and pressure-swing adsorption, and absorption[1-5]. In general, a gas separation membrane system is a pressure-driven, solution-diffusion process, where the basic mechanism for transport through dense membranes is sorption of a species into the membrane surface, diffusion across the membrane through a series of 'jumps' through the adjacent free volume elements, and desorption at the downstream of the membrane[6-8]. The performance of membrane materials for separating a given gas pair is typically characterized by two material dependent parameters: permeability and selectivity. High permeability, which can result from high fractional free volume (FFV) in polymers, can reduce the membrane area and the energy input required to process a given volume of gas; while high selectivity, which can result from size sieving and/or penetrant solubility selectivity, is important to improve separation efficiency [1, 5]. Ideally, gas separation membranes should have both high permeability and high selectivity. However, the performance of polymeric gas separation membranes is often limited by the trade-off relationship between permeability and selectivity proposed by Robeson via an empirical upper bound[9, 10]. Therefore, recent studies on polymer gas separation membranes have been largely focused on developing new macromolecular structures with high fractional free volume but narrow free volume distribution. A notable example includes thermally-rearranged polymers[11, 12] developed from *ortho*-functional polyimide precursors, which have shown outstanding gas permeation results, surpassing the 2008 upper bound. The success of thermally-rearranged polymers is ascribed to the very high fractional free volume and an optimized size distribution of free volume elements generated during molecular thermal rearrangement[11, 13-15]. Therefore, rational molecular design of polymers having high fractional free volume and well-controlled free volume architecture is often pursued to create new membranes with superior gas separation properties.

In this study, rigid, pinwheel-shaped triptycene molecules were judiciously incorporated into the backbone of polyimides to obtain polymers with high fractional free volume that is

tunable/controllable in size distribution. Triptycene, the simplest member of a large family of molecules known as iptycenes, is a rigid, bulky, three-dimensional shape-persistent moiety consisting of three symmetric benzene "blades" protruding from a single hinge[16-20], as shown in Figure 1. One of the defining characteristics of triptycene is the intrinsic open space between the benzene blades, known as internal free volume[20]. Additionally, when incorporated into a polymer backbone, triptycene functionality may hinder chain packing, resulting in intermolecular and intramolecular free volume elements that can affect gas transport. Due to the rigid, shape-persistent structure with 3-fold rotational symmetry, it is believed that the triptycene unit is a good component for the synthesis of polymers with high fractional free volume[21].

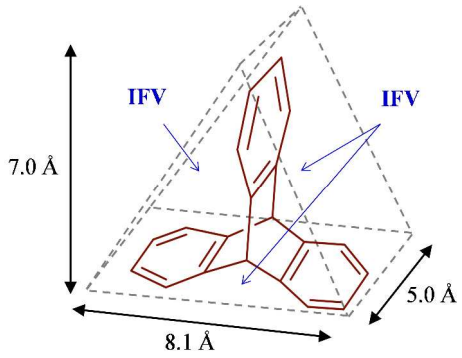

Figure 1: The triptycene molecule with high internal free volume (IFV)[20]

Because of the unique macromolecular structures induced by this bulky moiety, triptycene- and other iptycene-containing polymers have gained a lot of attention in the literature for various applications, such as low dielectric constant materials[19, 22, 23], polymer mechanical property enhancement[19, 20], gas adsorption[24, 25], and gas separations[21, 26, 27]. Of particular interest to this study is triptycene-containing polymers for gas separation membranes. Studied by Cho and Park, membranes prepared from the high fractional free volume 2,6-triptycene-polyimide showed a combination of high permeability and high selectivity, which placed its separation performance beyond the CO_2/N_2, H_2/N_2, and CO_2/CH_4 upper bounds[21]. Additionally, this polymer showed excellent resistance against CO_2 plasticization in a mixed-gas study. A more recent study describes the synthesis of two polymers of intrinsic microporosity (PIMs) which integrated triptycene units in the polyimide backbone[26]. Known as KAUST-PI-1 and KAUST-PI-2, these polymers were synthesized by incorporating triptycene with isopropyl groups substituted at the 9,10- position into a dianhydride and polymerizing with commercially available diamines.

These polymers showed excellent gas separation performance, exceeding the upper bound for O_2/N_2, H_2/N_2, H_2/CH_4, and CO_2/CH_4. Zhang et al. studied the effect of iptycenes on gas separation performance by synthesizing triptycene- and pentiptycene-containing poly[bis(benzimidazobenzisoquinolinones)]s. In their study the high free volume elements induced by the iptycenes allowed for high permeabilities with maintained high selectivities, especially for the pentiptycene-containing polymer[27]. The success of these studies provides strong incentives for continued work with triptycene-containing polymers in the area of gas separation membranes to provide fundamental understanding on the underlying molecular structure principles that control the polymer permeation properties to align with a specific gas separation. Therefore, it is the focus of this work to explore the idea of finely tuning gas transport properties of triptycene-containing polymers by careful variations to chemical structure to establish the fundamental structure-property relationship for this interesting family of polymer membrane materials.

Aromatic polyimides are good candidates for membrane-based gas separation applications due to their high glass transition temperature, rigid structure, thermal and mechanical stability, and proven gas separation performance[5]. In this study, a series of new polyimides containing the triptycene units were synthesized based on a set of newly designed triptycene diamines. In view of the significant effect of chemical structure on the gas transport properties, these triptycene-bearing polyimides were designed to systematically vary their substituent groups to investigate the possibility of tuning fractional free volume and subsequent gas transport properties. The series included an unsubstituted, *-para* linked triptycene polymer, a $–CH_3$ substituted polymer, and a $–CF_3$ substituted polymer. The methyl groups were selected because of their bulkiness. The trifluoromethyl groups were selected because of their chain-stiffening effect as well as their bulky nature, both of which lead to the disruption of chain packing resulting in higher fractional free volumes. Additionally CF_3 groups allow for improved solubility in casting solvents. The resulting triptycene-based polyimide membranes were comprehensively investigated for their chemical structures, thermal properties, density, fractional free volume, and gas permeation properties to elucidate the critical structural factors governing the transport behavior for this new series of polymers.

Experimental

Materials

Anthracene (97%), *p*-benzoquinone, and 1-fluoro-4-nitrobenzene were purchased from Aldrich and used as received. The aromatic dianhydride, 2,2'-bis-(3,4-dicarboxyphenyl) hexafluoropropane dianhydride (6FDA) was purchased from Akron Polymer Systems and thermally treated in vacuo at 180 °C overnight before use to cyclize possible *o*-diacid impurities. Xylenes, glacial acetic acid, hydrobromic acid (48%), *N,N*-dimethylformamide (DMF), hydrazine monohydrate, potassium carbonate, anhydrous *N,N*-dimethylacetamide (DMAc), pyridine, and acetic anhydride were purchased from Sigma-Aldrich and used as received. 1-fluoro-2-(trifluoromethyl)-4-nitrobenzene was purchased from Alfa Aesar, 1-chloro-2-methyl-4-nitrobenzene was purchased from TCI, and 1-methyl-2-pyrrolidinone (NMP) from Fischer Scientific, and were all used as received.

Synthesis of the triptycene-1,4-diamine monomers 4a-4c

A series of triptycene-1,4-diamine monomers (**4a-4c)** were synthesized via the reaction route shown in Scheme 1. The triptycene skeleton disubstituted with phenolic groups was first constructed via Diels-Alder cycloaddition reaction between anthracene and *p*-benzoquinone. The intermediate dinitro compounds (**3a-3c**) were obtained by the aromatic nucleophilic substitution (S_NAr) reactions between the triptycene diol (**2**) and an activated halogenated nitro compound (1-fluoro-4-nitrobenzene, 1-fluoro-2-(trifluoromethyl)-4-nitrobenzene, or 1-chloro-2-methyl-4-nitrobenzene), wherein the nitro groups were subsequently reduced to amines by Pd/C-catalyzed hydrazine reduction to afford corresponding triptycene-1,4-diamines (**4a-4c**).

Scheme 1: Synthesis of the triptycene-1,4-diamine monomers

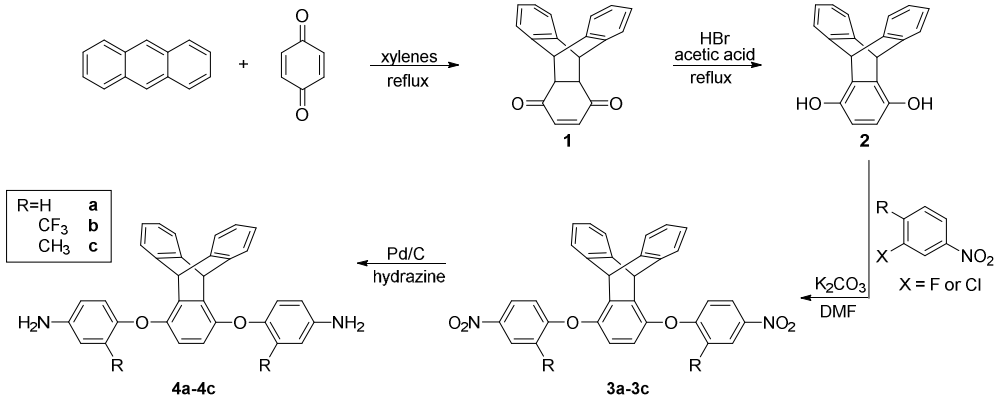

*Synthesis of triptycene-1,4-quinone (**1**) and triptycene-1,4-hydroquininone (**2**)*

Triptycene-1,4-quinone (**1**) and triptycene-1,4-hydroquinone (**2**) were prepared according to the published literature with some modifications[23]. A typical reaction is as follows: anthracene (10.12 g, 56.67 mmol), *p*-benzoquinone (7.37g, 68.14 mmol), and xylenes (70.8 mL) were added to a round-bottom flask with a stir bar. The mixture was refluxed at 140 °C with stirring under nitrogen atmosphere for six hours. The mixture was allowed to cool to room temperature and was filtered. The obtained solid was then washed three times in hot water (500 mL). The quinone product (**1**) (13.02 g, 80% yield) was collected and dried at 60 °C under vacuum overnight.

To synthesize triptycene hydroquinone (**2**), the quinone product (**1**) (13.02 g, 45.4 mmol) and glacial acetic acid (165 mL) were added to a round-bottom flask with a stir bar. The mixture was brought to reflux at 118 °C under nitrogen atmosphere. Hydrobromic acid (48%) (0.7 mL) was added to the flask and the mixture was allowed to reflux for an additional 30 minutes. A light tan precipitate was formed. The mixture was allowed to cool to room temperature and was then filtered. The resulting hydroquinone product (**2**) (11.71 g, 90% yield) was dried under vacuum at 60 °C for 9 hours.

*Synthesis of 1,4-bis(nitrophenoxy)triptycenes (**3a-3c**)*

The synthesis of 1,4-bis(nitrophenoxy)triptycene (**3a**) is used as an example to illustrate the detailed synthetic procedures. The hydroquinone product (**2**) (7.01 g, 24.5 mmol), dried potassium carbonate (7.46 g, 53.9 mmol), and DMF (80 mL) were added to a dry round-bottom flask with a stir bar. The mixture was allowed to stir at room temperature for 45 minutes. Next, 1-fluoro-4-nitrobenzene (6.92 g, 49.0 mmol) was added to the flask and the mixture was allowed to reflux at 153 °C under nitrogen atmosphere for 8 hours. The mixture was cooled to room temperature and was poured into 410 mL of a methanol/water mixture (1:1 by volume) to precipitate a light tan solid. The solid was collected via filtration and washed in methanol. The dinitro-*para* product (**3a**) was collected (8.15 g, 63% yield) and dried under vacuum at 100 °C overnight. It should be noted that a similar procedure was followed for the synthesis of the dinitro-CF_3 product (**3b**); however, a reflux temperature of 100 °C was used due to the low boiling temperature of 1-fluoro-2-(trifluoromethyl)-4-nitrobenzene. The reaction was monitored using thin layer chromatography (TLC) and the reaction was completed after refluxing for 3 hours. Additionally, the product was precipitated in the methanol/water mixture, and the precipitate was not washed. Likewise, for the synthesis of the dinitro-CH_3 product (**3c**), the

reflux temperature was 150 °C, and completion of the reaction was confirmed by TLC after 5 hours. The product was precipitated in a methanol/water mixture with no further washing.

*Synthesis of 1,4-bis(aminophenoxy)triptycenes (**4a-4c**)*

The synthesis of 1,4-bis(aminophenoxy)triptycene (**4a**) is used as an example to illustrate the detailed synthetic procedures. The dinitro-*para* product (**3a**) (5.25 g, 9.93 mmol), 10% Pd/C catalyst (0.27 g), and alcohol (210 mL) were added to a 500 mL round-bottom flask with a stir bar. The mixture was brought to reflux at 80 °C under nitrogen atmosphere. Hydrazine monohydrate (8.3 mL, 173.1 mmol) was added dropwise and the mixture was allowed to reflux for 8 h. The mixture was cooled to room temperature and the alcohol was removed under reduced pressure. DMF (16 mL) was then added to dissolve the product to facilitate filtration through packed Celite® to remove the catalyst. The filtered solution was precipitated in methanol (400 mL) and a fluffy, white solid was obtained. The diamine-*para* (**4a**) product was dried under vacuum at 110 °C for 22 h and stored in desiccator. A similar procedure was followed for the synthesis of the diamine-CF_3 (**4b**) and the diamine-CH_3 (**4c**) products with good yields; however, for (**4b**), the catalyst was removed simply by hot filtration directly after reflux and the product was recovered by removal of the alcohol under reduced pressure.

Synthesis of the triptycene-containing polyimides

Triptycene-containing polyimides were obtained via polycondensation reactions between the synthesized triptycene-1,4-diamines and 4,4'-(hexafluoroisopropylidene)diphthalic anhydride (6FDA), using the conventional chemical imidization method[28]. A sample polymerization is as follows: a three-neck flask equipped with a mechanical stirrer was flame-dried and allowed to cool to room temperature under nitrogen atmosphere. Diamine-*para* (**4a**) (1.6749 g, 3.57 mmol) was added to the flask, followed by anhydrous DMAc (16 mL). The diamine-*para* (**4a**) was allowed to dissolve at room temperature. Then the flask was submerged in an ice bath and 6FDA (1.5886 g, 3.57 mmol) was added as powder. The mixture was allowed to react in the ice bath for 6 hours to obtain a highly viscous poly(amic acid) solution. Then acetic anhydride (3 mL) was added to the poly(amic acid), followed by the addition of pyridine (3 mL), to promote chemical imidization. The mixture reacted for 20 h to ensure the formation of fully imidized polymer. The resulting highly viscous polyimide solution was diluted with a small amount of NMP before it was slowly precipitated and washed in stirring methanol (700 mL). The coagulated 6FDA-1,4-trip_*para* polyimide was collected via filtration and dried at 200 °C under vacuum for 24 h.

Similar procedures were followed for the synthesis of 6FDA-1,4-trip_CF_3 and 6FDA-1,4-trip_CH_3 polyimides. The structures of the polyimides are shown in Figure 2.

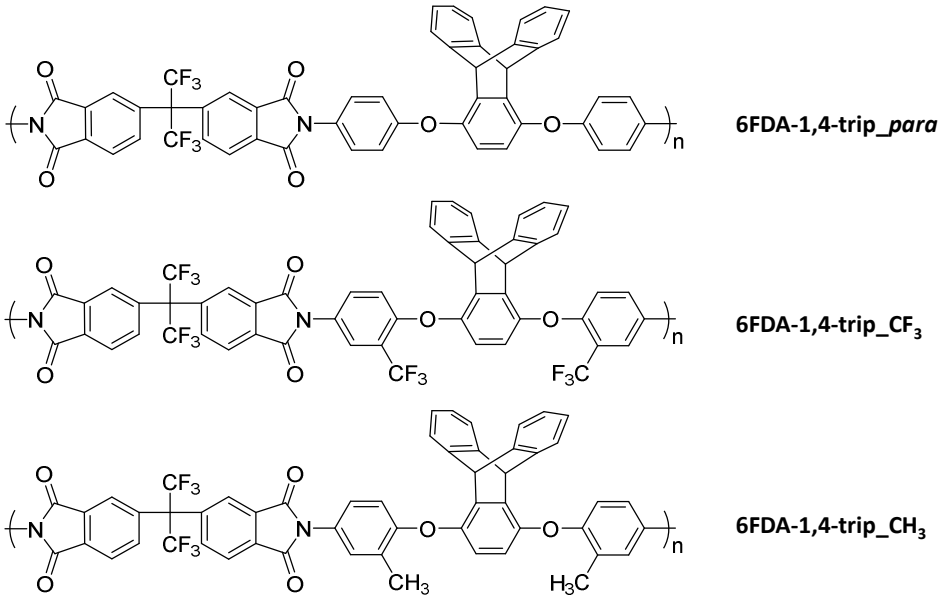

Figure 2: Series of 6FDA-1,4-triptycene polyimides

Characterization

^{1}H nuclear magnetic resonance (^{1}H NMR) experiments were conducted at room temperature on a Bruker 400 MHz or 500 MHz NMR spectrometer using DMSO-d_6 or $CDCl_3$ as a solvent.

Fourier transform infrared (FTIR) spectroscopy measurements were conducted using a Jasco FT/IR-6300 spectrometer with ATR on polymer thin films with a resolution of 1 cm^{-1} and 32 scans.

Differential scanning calorimetry (DSC) was performed with a Mettler Toledo DSC-1 in a nitrogen atmosphere at a heating rate of 10 °C/min. The glass transition temperature was taken as the midpoint of the change in slope of the baseline.

Thermal gravimetric analysis (TGA) was performed on a Mettler Toledo TGA/DSC-1. The fully-dried polymer film samples were evaluated over the range of 50-700 °C at a heating rate of 10 °C/min in an N_2 atmosphere.

Molecular weights of the synthesized polymers were determined by size exclusion chromatography (SEC) using a polystyrene standard at 35 ^{o}C in tetrahydrofuran.

Film Casting

Polymer dense films were cast using the following procedure. A solution of polyimide in NMP (~7%, w/v) was prepared. In some cases, heat was used to facilitate the dissolution. Then the solution was filtered using a 0.45 μm PTFE syringe filter to remove any impurities or undissolved particles. The filtered solution was spread as a thin layer onto a flat glass plate, which was dried with an IR lamp for ~24 h to remove most of the solvent and form the film. Next, the film was further dried at 200 °C under vacuum for ~24 h and removed from the plate. To ensure a solvent-free film, the film was soaked in methanol with slow stirring for 24 h to extract any residual NMP. The film was then dried once more at 200 °C under vacuum for ~24 h.

Density and Fractional Free Volume Determination

The fractional free volume (FFV) of each polymer was determined from Equation 1,

$$FFV = \frac{V - V_O}{V} \quad (1)$$

where V_O is the occupied volume of the polymer and V is the specific volume of the polymer (i.e., the inverse of the polymer density). Bondi's group contribution method was used to calculate the occupied volume, as shown in Equation 2,

$$V_O = 1.3 \sum V_{VDW} \quad (2)$$

where V_{VDW} is the van der Waals volume of each structural group in the polymer[29-31]. The density of a polymer film was determined experimentally using an analytical balance (ML204, Mettler Toledo) coupled with a density kit . In this method, the density of the sample is determined by Archimedes' principle by comparing the polymer's weight in air and in a liquid of known density, such as water, as shown in Equation 3,

$$\rho = \frac{A}{A-B}(\rho_w - \rho_a) + \rho_a \quad (3)$$

where A is the polymer weight in air, B is the polymer weight in water, ρ_w is the density of water, and ρ_a is the density of air[32]. Deionized water was chosen as the buoyant liquid due to its extremely low uptake (less than 0.3 wt%) in all film samples over the timescale of the experiment.

Pure Gas Permeability Measurements

The pure gas permeabilities (P, in barrers) of five gases (N_2, O_2, H_2, CO_2, and CH_4) were determined at 35 °C using a constant-volume variable-pressure method[33]. In this method, the flux of the permeate was determined by tracking the increase in pressure as a function of time into a

calibrated volume downstream of the polymer film[34, 35]. Permeability was calculated from Equation 4,

$$P_A = \frac{V_d l}{p_2 ART}\left[\left(\frac{dp_1}{dt}\right)_{ss} - \left(\frac{dp_1}{dt}\right)_{leak}\right] \quad (4)$$

where V_d is downstream volume, l is membrane thickness, p_2 is upstream absolute pressure, A is the area of film accessible to gas transport, R is the gas constant, T is temperature, and $(dp_1/dt)_{ss}$ and $(dp_1/dt)_{leak}$ are steady-state rates of pressure rise in the downstream volume at fixed upstream pressure and when the system is sealed under vacuum, respectively[33]. The ideal selectivity was determined by taking the ratio of the two species' pure gas permeabilities, as shown by Equation 5,

$$\alpha_{A/B} = \frac{P_A}{P_B} \quad (5)$$

where $\alpha_{A/B}$ is the selectivity of the gas pair in which A represents the more permeable gas[5].

Results and Discussion

Design and synthesis of triptycene-1,4-diamine monomers (4a-4c)

Triptycene monomers with primary amine groups are required for polyimide synthesis in diamine-dianhydride polycondensation reactions. The triptycene diamine monomers were designed to provide systematic variations in chemical structure that would affect gas transport. Amine groups were not directly introduced to the triptycene skeleton. Instead, an ether linkage was incorporated into the polymer backbone as a "spacer" to add chain flexibility, which could provide tough and ductile polyimide membranes with improved solubility and processability[36]. In addition to the base monomer (**4a**) with no further substituents, bulky substituent groups neighboring the triptycene unit (i.e., CH_3 and CF_3) were introduced, giving two new triptycene diamine monomers (**4b** and **4c**). The addition of the bulky side groups was expected to decrease chain-packing efficiency leading to higher fractional free volume and thus higher gas permeabilities. Moreover, the difference in size of the side groups was expected to possibly introduce more tunability control of the fractional free volume via partial "filling" the open space (internal free volume) between the benzene blades by the substituents. Therefore, these structural manipulations provide a new dimension in molecular design to finely tune the membrane properties of triptycene-containing polyimides. In addition, $–CF_3$ groups are known to improve solubility of aromatic polyimides.

The synthetic route to synthesizing a series of triptycene-1,4-diamine monomers (**4a-4c**) is shown in Scheme *1*. In this synthesis, a Diels-Alder reaction between anthracene and *p*-benzoquinone was used to construct the triptycene-1,4-quinone (**1**), which was subsequently converted to the triptycene-diol **(2)**. Next S_NAr reactions were used to obtain the intermediate dinitro compounds (**3a-3c**) which were reduced to the desired triptycene-1,4-diamines (**4a-4c**) using hydrazine catalyzed by Pd/C. The chemical structures of the synthesized diamines were confirmed by ^{1}H NMR as illustrated in Figure 3. As shown, each proton in the spectra can be unambiguously assigned according to the molecular structures of triptycene-1,4-diamines. Also, the clear assignment of the diamine monomers suggests they are of high purity, which is critical for successful condensation polymerizations to afford high molecular weight polyimides. This result was confirmed by the obtained high molecular polymers, which precipitated as long fibers.

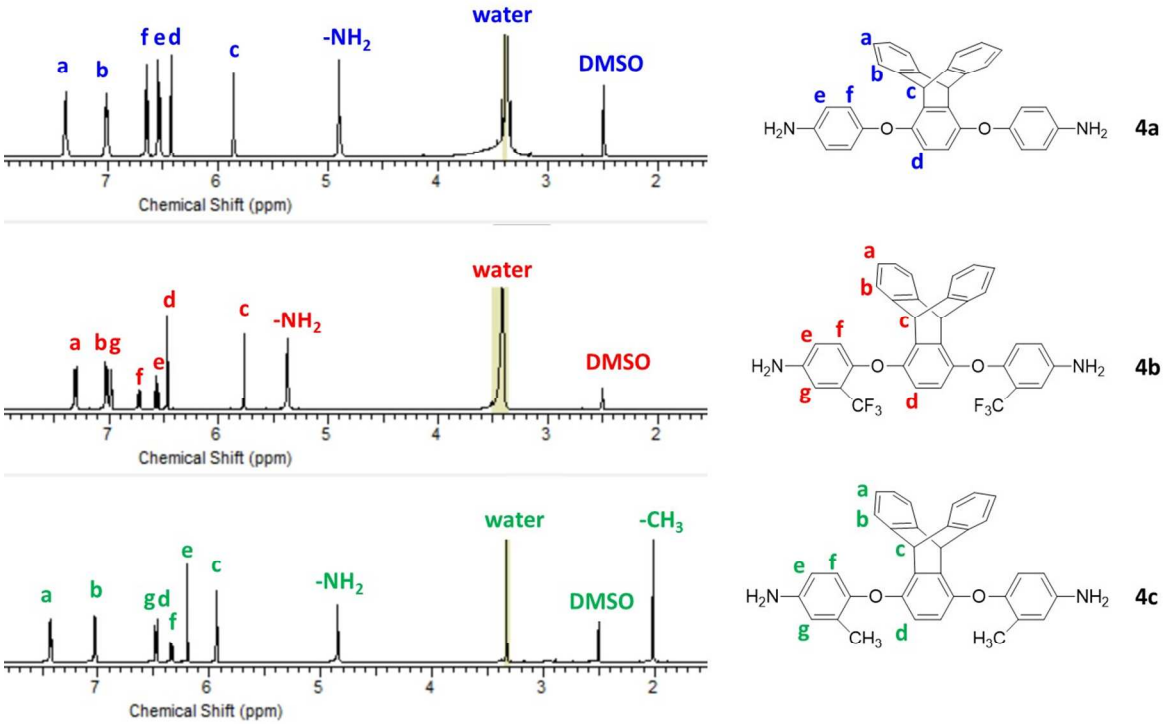

Figure 3: ^{1}H NMR of the triptycene-1,4-containing diamine monomers in DMSO-d_6

Synthesis and properties of triptycene-containing polyimides

A series of aromatic triptycene-containing polyimides (Figure 2) were prepared by polycondensation reaction of the triptycene-1,4-diamine monomer (**4a-4c**) with an aromatic dianhydride, 6FDA, in anhydrous DMAc as solvent and acetic anhydride and pyridine as

chemical imidization agents. The 6FDA-1,4-triptycene polyimides were obtained with fully imidized structure as confirmed by spectroscopy techniques. Figure 4 shows the FTIR spectra of the polyimides. The characteristic bands for the imide structure are identified as follows: asymmetric C=O stretching at 1780 cm^{-1}, symmetric C=O stretching at 1730 cm^{-1}, and C=O bending at 710 cm^{-1}. The fully imidized structure is confirmed by the absence of peaks in the 1620-1680 cm^{-1} range, which are indicative of poly(amic acid) carbonyl stretching.

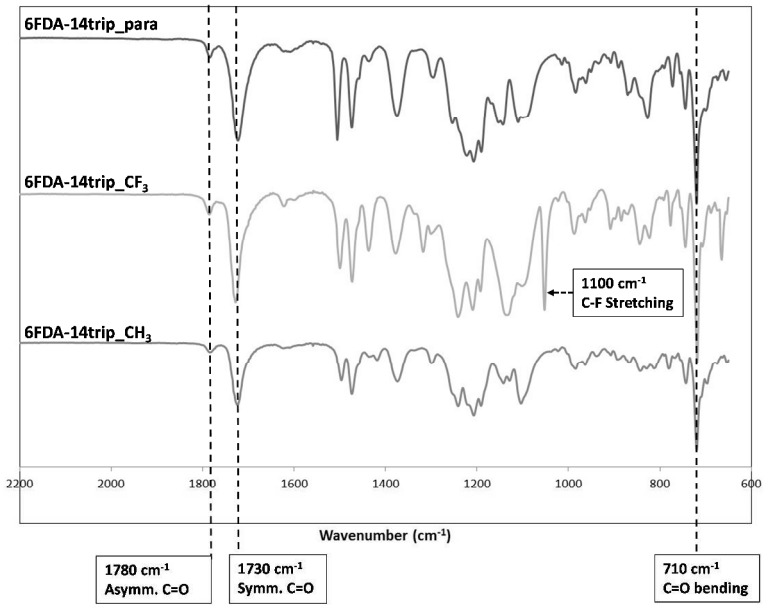

Figure 4: FTIR confirms fully imidized structure for the synthesized polyimides

The repeat unit structures of the triptycene-polyimides were also well supported by the ^{1}H NMR spectra, as shown in Figure 5. The spectra confirm the fully imidized structure, as indicated by the absence of poly(amic acid) proton peaks and clear proton assignment in accordance to the repeat unit structure. Within the resolution of the spectra, only peaks assigned to the polyimides were detected, which suggests high purity for the monomers.

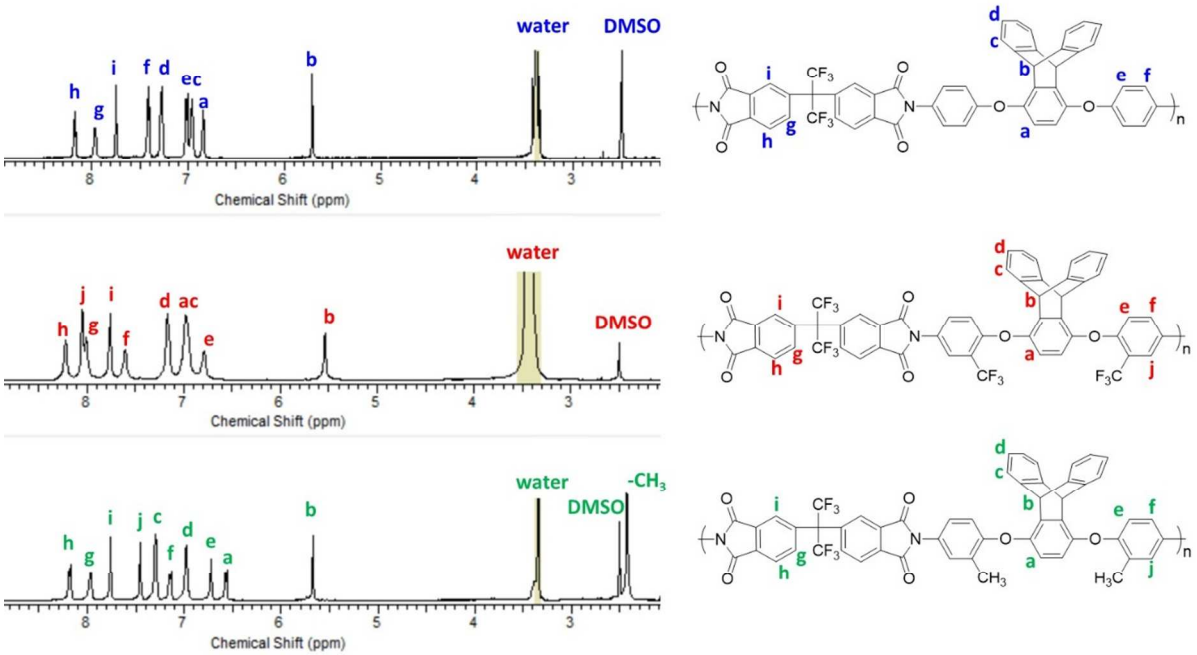

Figure 5: ^{1}H NMR of the 6FDA-1,4-triptycene polyimides in DMSO-d_6

The molecular weights and thermal properties of the synthesized 6FDA-1,4-triptycene polyimides were evaluated and are summarized in Table 1.

Table 1: Thermal properties of the 6FDA-1,4-triptycene polyimides

	M_n (g/mol) [a]	**PDI [a]**	**T_g (°C) [b]**	**$T_{d,\ 5\%}$ (°C) [c]**
6FDA-1,4-trip_*para*	4.18 x 10^4	3.01	300	528
6FDA-1,4-trip_CF_3	2.18 x 10^4	2.35	290	532
6FDA-1,4-trip_CH_3	3.44 x 10^4	2.50	280	518

[a] *SEC measurements in THF at 35 °C using polystyrene as reference*
[b] *DSC measurements: 10 °C/min, N_2*
[c] *TGA measurements: 10 °C/min, N_2; decomposition temperature T_d at 5% weight loss*

All the polyimides synthesized had sufficiently high molecular weights for film casting, ranging from ~20,000 to ~40,000 g/mol. Films were obtained from all the triptycene-polyimides synthesized via solution casting. Also, the polyimides exhibited excellent thermal properties with high glass transition temperatures (T_g) ranging from 280 °C to 300 °C. No melting/crystallization behavior was observed in the DSC measurements suggesting completely amorphous structures for all the triptycene-polyimides synthesized in this study. Polymers having high T_g values have

shown beneficial transport properties for a number of separations, such as hydrogen purification, natural gas sweetening, and nitrogen enrichments; additionally, rigid polymer chains facilitate in resisting the adverse effects of physical aging[5]. The substituted polymers had lower T_g values than the unsubstituted *para* polyimide, which likely indicates a reduction of intermolecular charge transfer complex (CTC) caused by the bulky substituent groups[23, 37]. Also, in the case of the CF_3 substitution, the bulky substituents disrupt chain packing, which contributes to an earlier onset of segmental motion, and consequently a lower T_g [38]. In comparing the two substituted polymers, the 6FDA-1,4-trip_CF_3 shows a higher T_g than the 6FDA-1,4-trip_CH_3, which can be attributed to the bulkier CF_3 moiety more effectively stiffening the polymer backbone than the CH_3 unit by introducing a barrier to segmental rotation. TGA traces revealed that all the polyimides in the series were thermally stable up to 500 °C without significant weight loss under air and nitrogen. The 5% weight loss temperatures for the triptycene-polyimides were in the range of 518–528 °C under nitrogen. All these polyimides showed high char yield, more than 59% (under nitrogen).

Solubility, Density and Fractional Free Volume (FFV)

Aromatic polyimides generally have poor solubility in common organic solvents due to strong inter-chain interactions of imide rings leading to poor processability. However, all the triptycene-containing polyimides synthesized in this study were found to have good solubilities in many organic solvents, as shown in Table *2*, allowing for facile film fabrication by solution casting and solvent evaporation. The much improved solubility of these polyimides is primarily due to the incorporation of the bulky triptycene units in the polymer backbone structure, which contain internal free volume elements and disrupt chain packing, allowing the solvents to enter into the material more easily. Noticeably, the 6FDA-1,4-trip_CF_3 sample can be readily dissolved in all the solvents tested except xylenes, in which it is partially soluble. The excellent solvent solubility is ascribed to the bulky fluorinated substituents in addition to the bulky triptycene moieties.

Table 2: Solubilities of triptycene polyimides in common organic solvents

	Solvents[a,b]									
	DMF	NMP	DMAc	DMSO	Toluene	Xylenes	THF	Acetone	DCM	Chloroform

6FDA-1,4-trip_CF_3	VS	VS	VS	VS	VS	PS	VS	VS	VS	VS
6FDA-1,4-trip_*para*	VS	S	S	S	S	NS	VS	PS	VS	VS
6FDA-1,4-trip_CH_3	VS	S	S	S	S	NS	VS	NS	VS	VS

[a]Solubility guide: VS=very soluble (at RT), S=soluble (heat of ≤100°C may be required), PS=partially soluble (incomplete dissolution even with heat of ≤100°C), NS=not soluble (insoluble even with heat of ≤100°C)
[b]For all solvents tested, an approximate concentration of 0.01 g/mL was used.

Table 3 lists the measured densities and calculated fractional free volume values of the triptycene-polyimides synthesized. For comparison, density and fractional free volume data for other reported 6FDA-based polyimides, the commercial Matrimid® polyimide, and a few select "high-free-volume" glassy polymers are also presented.

Table 3: Density and fractional free volume (FFV) of the 6FDA-1,4-triptycene polyimides

	Density (g/cm^3)*	**V_W (cm^3/mol)**	**V_O (cm^3/mol)**	**FFV (%)**
6FDA-1,4-trip_CH_3	1.323 ± 0.002	445.03	578.54	15.1
6FDA-1,4-trip_*para*	1.349 ± 0.006	420.89	547.16	15.6
6FDA-1,4-trip_CF_3	1.381 ± 0.002	460.29	598.38	18.3
6FDA-APAF[13]	1.536	-	-	15.9
6FDA-HAB[12]	1.407	-	-	15.0
Matrimid®[5, 39]	1.175	-	-	17
PTMSP[40]	0.61-0.83	-	-	32-34
PIM-1[5, 41]	1.06-1.09	-	-	22-24

* Uncertainties were calculated as the standard deviation of at least three repeat measurements

As shown in Table 3, the other 6FDA-based polyimides from the literature have higher densities than those of the triptycene-containing polyimides, which were all below 1.40 g/cm^3. This result further indicates evidence of the poor chain packing efficiency due to the incorporation of the bulky triptycene units in the polymer backbones. The densities of the triptycene-polyimide series increase when the substituent is changed from –CH_3, to –*para*, to –CF_3. The high density of the 6FDA-1,4-trip_CF_3 polymer can be explained by the relatively

heavy substituent CF_3 groups. Free volume properties (i.e., fractional free volume and free volume size distribution) play a critical role in polymer membrane gas separation processes that are governed by the solution-diffusion mechanism. High fractional free volume allows for high diffusivities of a penetrant through the material, which in combination with the penetrants' solubility, determines the permeability in the polymer. For high selectivity, a narrow size distribution of free volume elements is required. As shown in Table 3, the synthesized triptycene-containing polyimides exhibited relatively high fractional free volume, as was expected due to the incorporation of the bulky, shape-persistent triptycene units. For example, the fractional free volume of the 6FDA-1,4-trip_CF_3 sample surpassed that of Matrimid® polyimide, which is known for its good permeability, especially with regards to CO_2, among commercial polymers[5]. The triptycene polymers had lower fractional free volume than certain "high-free-volume" polymers; however, all of the polymers considered in this study had fractional free volume values that are consistent with those of other polyimides of commercial and academic interest. Thus, there is promise for continued work in the area of triptycene-containing polyimides for high fractional free volume polymers.

It is important to notice that the free volume for the triptycene-polyimide series changed by modifying the substituent groups (–H, $–CH_3$ and $–CF_3$) neighboring the triptycene units. The addition of bulky substituent groups usually disrupts chain packing due to steric hindrances and chain-stiffening, which would in turn increase the fractional free volume and the permeability[14, 42-44]. Typically, the fractional free volume of the polymer membrane increases as the bulkiness of the side group increases. While this trend was observed for the $–CF_3$ substituted polymer, it was not observed in the case of the $–CH_3$ substituted one. Instead, a decrease in fractional free volume was observed in the 6FDA-1,4-trip_CH_3 polyimide compared to the 6FDA-1,4-trip_*para* sample. This result could be attributed to the size difference of the substituent groups and the unique configuration of the triptycene moiety along the backbone. In comparing the occupied volumes (V_0) of the side groups, the trifluoromethyl moiety's occupied volume (46.0 $Å^3$) is 56% larger than that of the methyl group (29.5 $Å^3$)[30]. Within the triptycene-polyimide films, the majority of the void space originates from the cumulative effect of increased inter-chain spacing induced by the bulky triptycene blades protruding from the polymer backbone, as well as the internal free volume associated with triptycene units (refer to Figure 1). In the case of the large –CF_3 moieties, the bulky side groups add to the disruption of chain packing, creating more and/or

larger void space than is normally seen in other polymer systems. However, it is likely that since the methyl groups are relatively small in size, a significant portion of them might reside partially in the void space (internal free volume) of triptycene clefts, which is approximately 31.0 $Å^3$ in volume per cleft based on Tsui et al.'s work[20]. As a result it causes a decrease in the fractional free volume as compared with the 6FDA-1,4-trip_*para* polyimide. The proposed chain packing mechanism is schematically depicted in Figure 6. Additionally, the CH_3 substitution has less pronounced chain-stiffening effect compared to that of the CF_3 substitution, which may also contribute to the differences in fractional free volume. This interpretation is supported by the lower glass transition temperature of the 6FDA-1,4-trip_CH_3 compared to that of the 6FDA-1,4-trip_CF_3 (Table 1). Moreover, the addition of the trifluoromethyl group is more effective in lowering the CTC than the methyl group due to its larger size and electron-withdrawing nature[37]. The reduced CTC will lead to less efficient chain packing and thus increased fractional free volume.

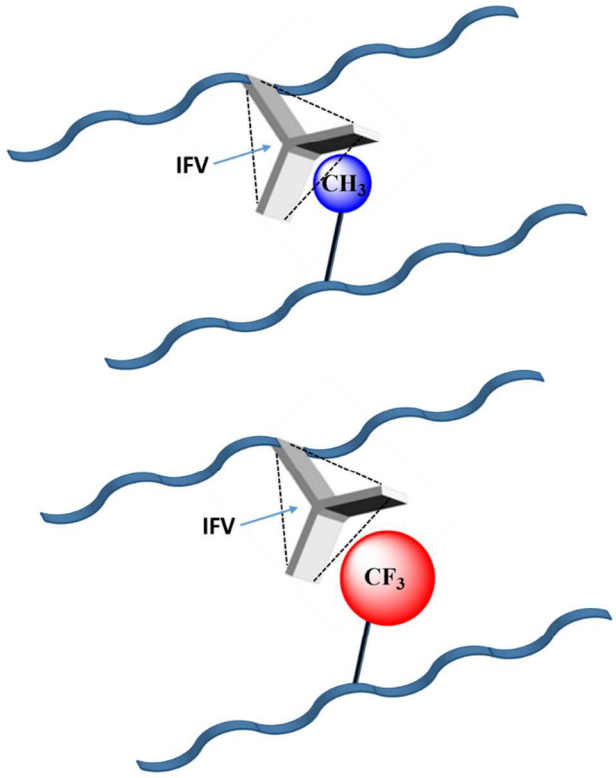

Figure 6: Possible packing mechanism of the CF_3 and CH_3 moieties with regards to the triptycene unit

Gas Transport Properties

Using a constant-volume, variable-pressure method, the triptycene-containing polyimide permeabilities to pure H_2, CO_2, O_2, N_2, and CH_4 were determined[34]. For these measurements, the polymer films were carefully measured in their thickness and test area. The film thickness was in a range of 30-40 μm with approximate test area of 1 cm^2. To the best of our knowledge, gas transport properties of triptycene-1,4-polyimides have not been reported in the open literature. The permeability coefficients as a function of feed pressure are shown in Figure 7 for these triptycene-polyimide membranes.

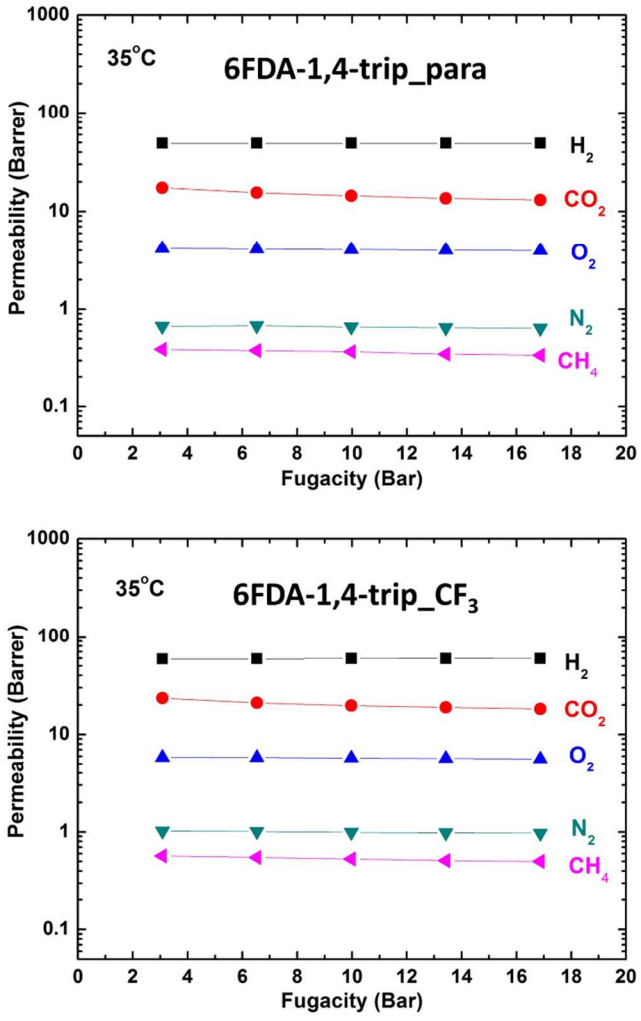

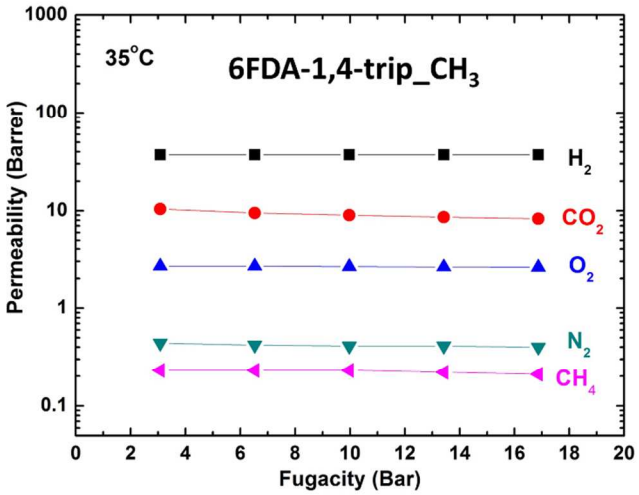

Figure 7: Pure gas permeability of the triptycene-polyimides as a function of feed pressure

For all polymers in this study, their permeabilities followed the order of: $P(H_2) > P(CO_2) > P(O_2) > P(N_2) > P(CH_4)$, which is consistent with the kinetic diameters of the penetrant gas molecules, indicating that diffusion selectivity plays an important role in these polymers. The feed pressure had very little effect on the permeability. Especially noteworthy are the CO_2 permeabilities, which are often affected due to membrane plasticization; however, for all samples considered in this study, CO_2 permeability decreased with increasing fugacity up to 17 atm, which is consistent with dual-mode sorption and no plasticization pressure point[5, 45]. Because there was little change in the permeability values above 10 atm (130 psig), the following analyses of gas transport properties will use values measured at 10 atm. More specifics on the 6FDA-1,4-triptycene polyimides gas transport properties, along with three commercially-available glassy polymers for comparison, are listed in Table 4.

Table 4: Pure gas transport properties of the 6FDA-1,4-triptycene polyimides

	Gas Permeability (Barrer) at 35°C & 130 psig				
	CO_2	**O_2**	**H_2**	**N_2**	**CH_4**
6FDA-1,4-trip_CF_3	19.7	5.75	59.4	0.99	0.53
6FDA-1,4-trip_*para*	14.4	4.07	49	0.66	0.37
6FDA-1,4-trip_CH_3	9.0	2.64	37	0.41	0.23
Matrimid®[5]	10	2.1	18	0.32	0.28

Polysulfone[46, 47]	5.6	1.20	-	0.18	0.18
Polycarbonate[46, 48]	6.0	1.48	-	0.26	0.28
	Ideal Selectivity at 35°C & 130 PSIG				
	CO_2/CH_4	**O_2/N_2**	**CO_2/N_2**	**H_2/N_2**	**H_2/CH_4**
6FDA-1,4-trip_CF_3	37	5.8	20	60	113
6FDA-1,4-trip_*para*	39	6.0	22	74	132
6FDA-1,4-trip_CH_3	39	6.4	22	90	161
Matrimid®[5]	36	6.6	31	56	64
Polysulfone[46, 47]	22	6	31	-	-
Polycarbonate[46, 48]	23	5	23	-	-

As shown in Table 4, all three synthesized triptycene-containing polyimides had higher permeabilities than polysulfone and polycarbonate for all five gases. In addition, triptycene-based polyimides also outperformed selectivity in most cases. The triptycene polyimides also had generally higher gas permeabilities than Matrimid® polyimide. For example, the CO_2 and CH_4 permeabilities of 6FDA-1,4-trip_CF_3 membrane almost doubled those of the Matrimid® polyimide and O_2, N_2 and H_2 permeabilities were tripled. Moreover, these triptycene polyimides simultaneously showed very comparable selectivities to Matrimid® polyimide with some of the selectivities being higher than those of Matrimid®. This is very promising as the permeability/selectivity trade-off generally prevents improved properties in both permeability and selectivity for common polymeric membranes. Another important observation from Table 4 is that the transport properties of the triptycene-polyimides are very sensitive to changes in the substituents in the monomer structure, which are related to the amount of the free volume elements imparted by them. As shown, the permeabilities of the triptycene-polyimides increased from the –CH_3, to the –*para*, to the –CF_3 substitution. This nicely agreed with the fractional free volume values obtained for this set of polymers, which is expected from free volume theory[49] because, as the free volume within the polymer increases, there is more available space through which the gas molecules can diffuse. Previous studies[50] have shown an approximate correlation between gas permeability, P, and fractional free volume, FFV, by the following equation:

$$P = Ae^{\frac{-B}{FFV}} \quad (6)$$

where A and B depend on temperature and gas type, respectively. A semilogarithmic plot of gas permeability vs. inverse of fractional free volume is shown in Figure 8.

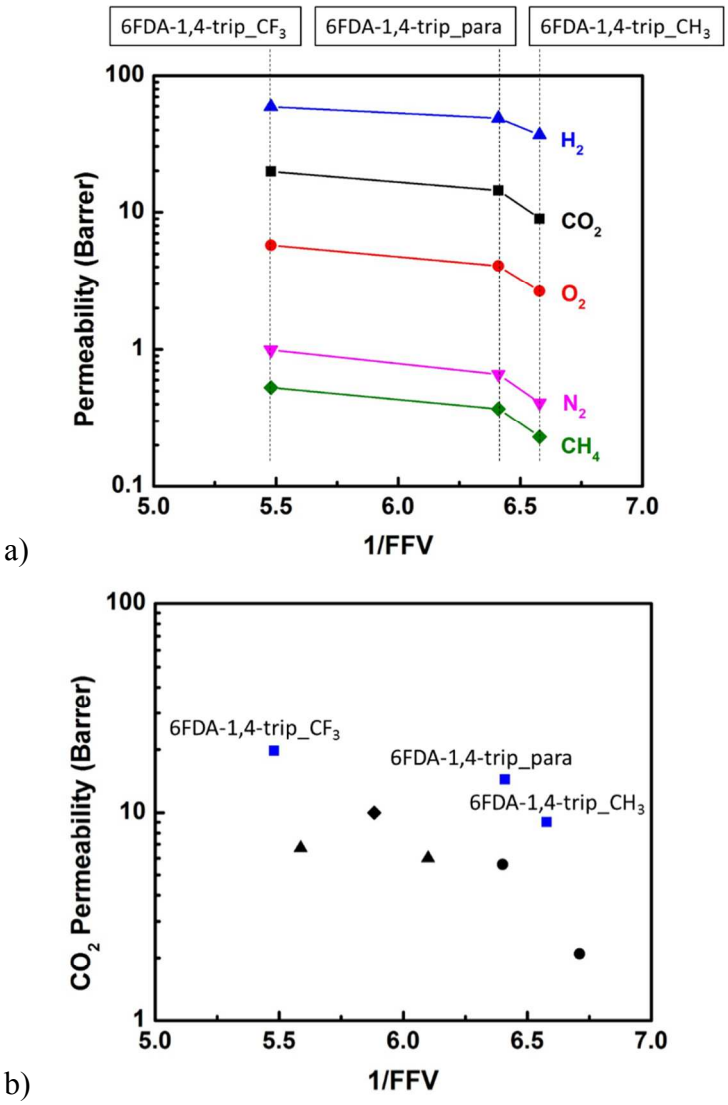

Figure 8: (a) Relationship between gas permeability and fractional free volume (FFV) for triptycene-polyimides; (b) Comparison of the dependence of CO_2 permeabilities on fractional free volume for the triptycene-polyimides (■), polycarbonates[48] (▲), Matrimid®[5](♦), and polysulfones[47] (●)

As shown in Figure 8 (a), the increase in fractional free volume accompanied with the increase in the gas permeability for all the gases tested. This increasing trend of the permeability's dependence on the fractional free volume clearly shows that the gas permeability can be feasibly tuned by altering the polymer structure, or specifically in this study, the substituents neighboring the triptycene moieties. A closer look at the dependence of CO_2

permeability on fractional free volume for these polyimides is shown in Figure 8 (b) along with data for two polysulfones[47], Matrimid®[5], and two polycarbonates[48]. Interestingly, even for similar fractional free volume values (e.g., 6FDA-1,4-trip_*para* vs. polysulfone), triptycene polyimides showed much higher permeability, suggesting favorable free volume size distribution in these triptycene-containing polyimide membranes. Another possibility for the higher permeability of the 6FDA-1,4-trip_*para* polymer compared to polysulfone could be due to increased gas solubilities induced by the $-C(CF_3)_2$ group in the 6FDA unit compared to the unfluorinated polysulfone structure[45], which could be confirmed by determination of gas solubilities and diffusivities of the triptycene-containing polymers. However, the interpretation of favorable free volume size distribution again explains the high ideal selectivities exhibited by the 6FDA-1,4-triptycene polyimides in combination with their high permeabilities (Table 4). The configurational symmetry of triptycene unit and its noncompliant feature may allow for the formation of rather uniform free volume elements throughout the polymers, potentially facilitating improved size sieving capabilities. Additionally, it can be seen that the introduction of the substituent groups led to subtle differences in the selectivities in this series of polymers. As previously discussed, it is suggested that the $-CH_3$ moieties might partially fill the empty space created by the triptycene unit, reducing free volume. This increased packing density could allow for increased sieving capabilities and thus higher selectivities when compared to the *–para* polyimide. Likewise, the $-CF_3$ substituted polymers showed slightly lower selectivities in comparison to the *–para* polyimide, which is consistent with disruptions to chain packing and higher fractional free volume. The substituent effect on selectivities and permeabilities indicates the tunability of the gas transport properties by tailoring the chemical structure of the triptycene-containing polyimides. Particularly, the unique internal free volume feature (Figure 1) of the triptycene-containing polyimides adds a new dimension in chain packing driving force at the molecular level that would allow facile manipulation of chain organization to construct tailored free volume architecture, thus promoting fast transport and selective separations.

The permselectivity for CO_2/CH_4 gas pair vs. $P(CO_2)$ and permselectivity for O_2/N_2 gas pair vs. $P(O_2)$ of the 6FDA-1,4-triptycene polyimides are plotted in the Robson upper bound as shown in Figure 9. The three synthesized polyimides showed promising results, all positioned near the upper bound. These results can be primarily attributed to the incorporation of the bulky, symmetric triptycene unit, which efficiently disrupted chain-packing and created large amounts

of relatively uniform free volume elements. This allowed for fast transport, while maintaining high selectivities. Despite these polymers residing below the upper bound, modifications to the polymer backbone and thus the free volume architecture do not result in permeabilities and selectivities that parallel the upper bound; instead, property sets move rather laterally approaching the upper bound. Therefore, if the triptycene-polymer structure undergoes further judicious modification, it may be possible to further advance the membrane performance along this more horizontal trend and potentially cross the upper bound.

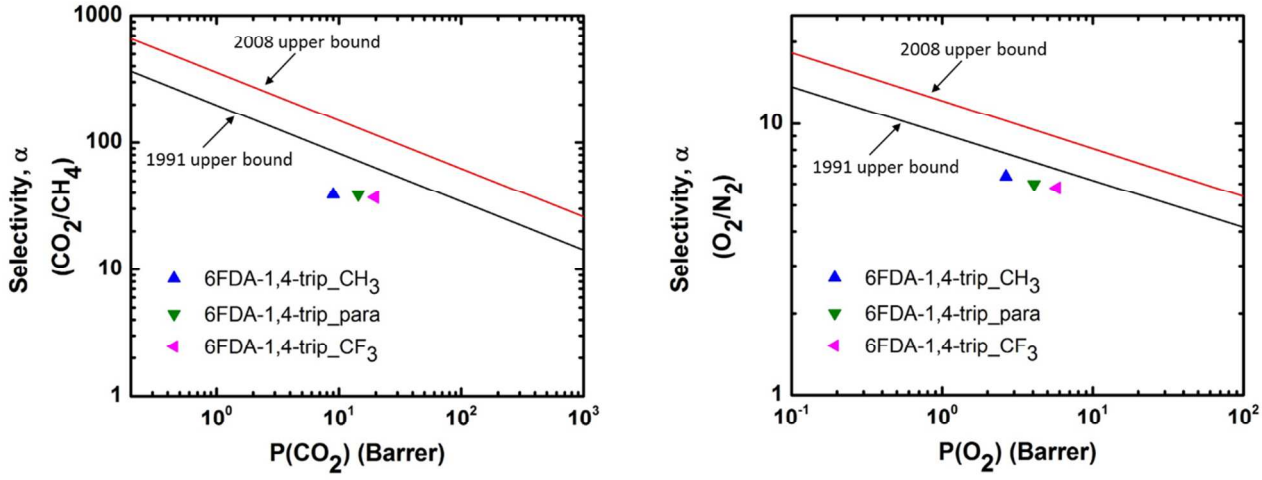

Figure 9: Permeability/selectivity trade-off tuned by chemical structure

Conclusions

A series of three 1,4-triptycene diamines with systematically varied substituted groups were synthesized with high purity. These diamines were successfully polymerized with commercially-available 6FDA to obtain a series of triptycene-containing polyimides with high molecular weight. These triptycene-containing polyimides showed good solubility in various organic solvents as well as excellent thermal properties due to the presence of bulky triptycene moieties in the polymer backbone, which made them suitable for further investigation of gas transport properties. The triptycene-polyimides had high fractional free volume, which naturally led to high gas permeabilities, particularly when compared to several commercial glassy polymer gas separation membranes. High selectivities were also observed for these 1,4-triptycene polyimides, which can be attributed to favorable free volume size distribution induced by the symmetric nature of the triptycene unit. A correlation between fractional free volume and gas

transport properties was evaluated, suggesting that further manipulation of the polymer chemical structure could allow for fine-tuning of the gas permeation properties and result in polyimides which could perform above the upper bound. Possible directions for continued work with these polymers include sorption testing for fundamental permeation properties, measurement of d-spacing for more information on chain packing, and physical aging experiments to determine the long term stability of these polymer membranes. Additionally, more research in this area is being carried out to produce additional newly-designed triptycene-containing polyimides with potential to achieve superior gas separation performance.

Acknowledgements

The authors would like to acknowledge the support of the Division of Chemical Sciences, Biosciences, and Geosciences, Office of Basic Energy Sciences of the U.S. Department of Energy (DOE) under Award DE-SC0010330. The project was also supported in part by the Center of Sustainable Energy at Notre Dame (cSEND).

References

1 P. Bernardo, E. Drioli and G. Goelmme, *Ind. Eng. Chem. Res.,* 2009, **48**, 4638.
2 R. Baker, *Ind. Eng. Chem. Res.,* 2002, **41**, 1393-1411.
3 P. Budd and N. McKeown, *Polym. Chem.,* 2010, **1**, 63-68 .
4 V. Abetz, T. Brinkmann, M. Dijkstra, K. Ebert, D. Fritsch, K. Ohlrogge, D. Paul, S. Pereira Nunes, N. Scharnagl and M. Schossig, *Advanced engineering materials,* 2006, **8**, 328-358.
5 D. F. Sanders, Z. P. Smith, R. Guo, L. M. Robeson, J. E. McGrath, D. R. Paul and B. D. Freeman, *Polymer,* 2013, **54**, 4729.
6 A. Fick, *J. Membr. Sci.,* 1995, **100**, 33-38.
7 T. Graham, *J. Membr. Sci.,* 1995, **100**, 27-31.
8 J. Wijmans and R. Baker, *J. Membr. Sci.,* 1995, **107**, 1-21.
9 L. M. Robeson, *J. Membr. Sci.,* 1991, **62**, 165.
10 L. M. Robeson, *J. Membr. Sci.,* 2008, **320**, 390.
11 H. B. Park, C. H. Jung, Y. M. Lee, A. J. Hill, S. J. Pas, S. T. Mudie, E. Van Wagner, B. D. Freeman and D. J. Cookson, *Science,* 2007, **318**, 254-258
12 D. F. Sanders, Z. P. Smith, C. P. Ribeiro Jr., R. Guo, J. E. McGrath, D. R. Paul and B. D. Freeman, *J. Membr. Sci.,* 2012, **409**, 232-241.
13 H. Park, S. Han, C. Jung, Y. Lee and A. Hill, *J. Membr. Sci.,* 2010, **359**, 11-24.
14 R. Guo, D. Sanders, Z. Smith, B. Freeman, D. Paul and J. McGrath, *J. Mater. Chem. A,* 2013, **1**, 262-272.

15 S. H. Han, H. Kwon, K. Kim, J. Seong, C. Park, S. Kim, C. M. Doherty, A. W. Thornton, A. J. Hill, A. E. Lozano, K. A. Berchtold and Y. M. Lee, *Phys. Chem. Chem. Phys,* 2012, **14**, 4365-73.
16 P. D. Bartlett, M. J. Ryan and S. G. Cohen, *J. Am. Chem. Soc.*, 1942, **64**, 2649.
17 E. Hoffmeis, J. Kropp, T. McDowell, R. Michel and W. Rippie, *J. Pol. Sci. Part A. Pol. Chem.,* 1969, **7**, 55.
18 A. Bashir-Hashemi, H. Hart and D. L. Ward, *J. Am. Chem. Soc.*, 1986, **108**, 6675.
19 T. M. Swager, *Acc. Chem. Res.,* 2008, **41**, 1181.
20 N. T. Tsui, A. J. Paraskos, L. Torun, T. M. Swager and E. L. Thomas, *Macromolecules,* 2006, **39**, 3350-3358 .
21 Y. J. Cho and H. B. Park, *Macromol. Rapid Commun.,* 2011, **32**, 579.
22 S. A. Sydlik, Z. Chen and T. M. Swager, *Macromolecules,* 2011, **44**, 976.
23 S. Hsiao, H. Wang, W. Chen, T. Lee and C. Leu, *Pol. Sci. Part A. Pol. Chem,* 2011, **49**, 3109.
24 B. S. Ghanem, M. Hashem, K. D. M. Harris, K. J. Msayib, M. Xu, P. M. Budd, N. Chaukura, D. Book, S. Tedds, A. Walton and N. B. McKeown, *Macromolecules,* 2010, **43**, 5287-5294.
25 C. Zhang, Y. Liu, B. Li, B. Tan, C. Chen, H. Xu and X. Yang, *ACS Macro. Lett.,* 2012, **1**, 190-193.
26 B. S. Ghanem, R. Swaidan, E. Litwiller and I. Pinnau, *Adv.Mater.,* 2014, DOI:10.1002/adma.201306229.
27 H. Mao and S. Zhang, *Polymer,* 2014, **55**, 102-109.
28 H. Ohya, V. V. Ohya and S. I. Kudryavtsev, *Desalination,* 1997, **109**, 225-225
29 A. Bondi, *J. Phys. Chem.,* 1964, **68**, 441.
30 D. W. van Krevelen and K. te Nijenhuis, in *Properties of Polymers*, ed. anonymous, Elsevier Science, 2009, p. 71.
31 J. Y. Park and D. R. Paul, *J. Membr. Sci.,* 1997, **125**, 23.
32 *Density Kit For Solids and Liquids Determination Operating Instructions,* Mettler Toledo.
33 *Springer Handbook of Material Measurement Methods*, ed. H. Czichos, T. Saito and L. Smith, Springer Science and Business Media, 2006, p. 283.
34 H. Lin and B. D. Freeman, in *Springer handbook*, ed. H. Czichlos, T. Saito and L. Smith, Springer, New York, 2006, p. 371-387.
35 Z. P. Smith, R. R. Tiwari, M. E. Dose, K. L. Gleason, T. M. Murphy, D. F. Sanders, G. Gunawan, L. M. Robeson, D. R. Paul and B. D. Freeman, *Macromolecules,* 2014, *in press.*, DOI: 10.1021/ma402521h.
36 J. Espeso, A. E. Lozano, J. G. de la Campa and J. de Abajo, *J. Membr. Sci.,* 2006, **280**, 659-665.
37 C. Yang, R. Chen and K. Chen, *J. Pol. Sci. Part A. Pol. Chem.,* 2003, **41**, 922-938.
38 F. Li, S. Fang, J. Chen, J. J. Ge, P. S. Honigfort and F. W. Harris, *Polymer,* 1999, **40**, 4571-4583.
39 S. Basu, A. Cano Odena and A. Cano-Odena, *J. Membr. Sci.,* 2010, **362**, 478-487.
40 L. Starannikova, V. Khodzhaeva and Y. Yampolskii, *J. Membr. Sci.,* 2004, **244**, 183-191.
41 N. Y. Du, G. P. Robertson, I. Pinnau and M. D. Guiver, *Macromolecules*, 2010, **43**, 8580.
42 D. F. Sanders, R. Guo, Z. P. Smith, Q. Liu, K. A. Stevens, J. E. McGrath, D. R. Paul, and B. D. Freeman, *Polymer,* 2014, **55**, 1636-1647.

43 C. Nagel, K. Gunther Schade, D. Fritsch, T. Strunskus, F. Faupel and K. Günther Schade, *Macromolecules,* 2002, **35**, 2071-2077.
44 S. Huang, C. Hu, K. Lee, D. Liaw and J. Lai, *European Polymer Journal,* 2006, **42**, 140-148.
45 S. T. Matteucci, Y. P. Yampolskii, B. D. Freeman and I. Pinnau, in *Materials science of membranes for gas and vapor separation*, ed. Y. Yampolskii, I. Pinnau and B. D. Freeman, John Wiley & Sons, Chichester, 2006, p. 1-47.
46 W. J. Koros, G. K. Fleming, S. M. Jordan, T. H. Kim and H. H. Hoehn, *Prog. Polym. Sci.,* 1988, **13**, 339.
47 J. S. McHattie, W. J. Koros and D. R. Paul, *Polymer,* 1991, **32**, 840-850.
48 N. Muruganandam, W. J. Koros and D. R. Paul, *J. Pol. Sci. Part B. Pol. Phys.,* 1987, **25**, 1999-2026.
49 M. Cohen and D. Turnbull, *J. Chem. Phys.,* 1959, **31**, 1164-1169.
50 M. R. Pixton and D. R. Paul, *Macromolecules,* 1995, **28**, 8277-8286.

Graphic Abstract

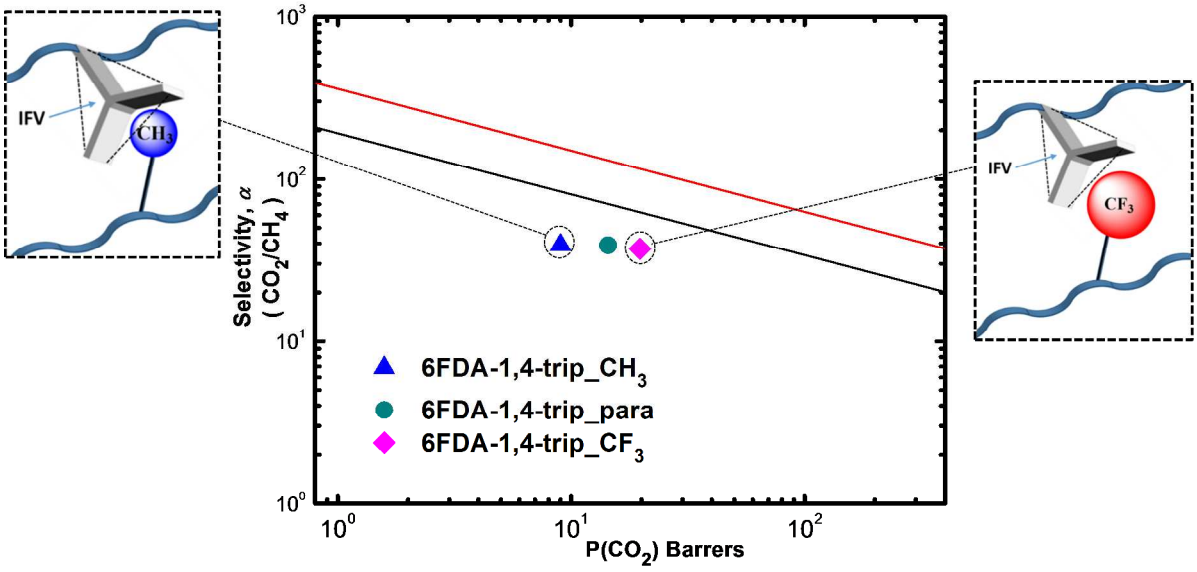

Triptycene-containing polyimide membranes with tunable fractional free volume promoting fast gas transport and selective separations